DE GRUYTER Z. Phys. Chem. 2016; 230(9): 1219–1231

Francesco Armetta, Motshabi A. Sibeko, Adriaan S. Luyt, Delia F. Chillura Martino, Alberto Spinella, and Maria Luisa Saladino*

Influence of the Ce:YAG Amount on Structure and Optical Properties of Ce:YAG-PMMA Composites for White LED

DOI 10.1515/zpch-2015-0703
Received October 13, 2015; accepted March 13, 2016

Abstract: Ce:YAG-poly(methyl methacrylate) (PMMA) composites were prepared by using a melt compounding method, adding several amounts of Ce:YAG in the range 0.1–5 wt. %. The optical properties of the obtained composites and of the composites combined with a blue LED were measured to investigate the effect of the amount of Ce:YAG on the resulting emitted light in view of possible application in white LED manufacture. An increase in Ce:YAG amount caused an increase in the emission and a shift of 15 nm, influencing the white LED performance. The structure and morphology of the composites were studied. The results show that the interaction between the two components, observed by using solid state NMR experiments, are the responsible for the observed shift.

***Corresponding author: Maria Luisa Saladino,** Dipartimento Scienze e Tecnologie Biologiche, Chimiche e Farmaceutiche – STEBICEF and INSTM UdR – Palermo, Università di Palermo, Parco d' Orleans II, Viale delle Scienze pad.17, Palermo I-90128, Italy; and Centro Grandi Apparecchiature-ATeN Center, Università di Palermo, Via F.Marini 14, Palermo I-90128, Italy, e-mail: marialuisa.saladino@unipa.it
Francesco Armetta: Dipartimento Scienze e Tecnologie Biologiche, Chimiche e Farmaceutiche – STEBICEF and INSTM UdR – Palermo, Università di Palermo, Parco d' Orleans II, Viale delle Scienze pad.17, Palermo I-90128, Italy; and Centro Grandi Apparecchiature-ATeN Center, Università di Palermo, Via F.Marini 14, Palermo I-90128, Italy
Delia F. Chillura Martino: Dipartimento Scienze e Tecnologie Biologiche, Chimiche e Farmaceutiche – STEBICEF and INSTM UdR – Palermo, Università di Palermo, Parco d' Orleans II, Viale delle Scienze pad.17, Palermo I-90128, Italy
Alberto Spinella: Centro Grandi Apparecchiature-ATeN Center, Università di Palermo, Via F.Marini 14, Palermo I-90128, Italy
Motshabi A. Sibeko: Department of Chemistry, University of the Free State (Qwaqwa Campus), Private Bag X13, Phuthaditjhaba, 9866, South Africa
Adriaan S. Luyt: Center for Advanced Materials, Qatar University, PO Box 2713, Doha, Qatar

Keywords: Polymeric Composites, Ce:YAG, PMMA, White LED, Interface Interactions.

1 Introduction

After nearly a century of rapid development, LEDs are considered by the scientific community as being ready to replace incandescent and fluorescent lighting. The definition of the relevant factors that affect the quality of these new sources is a key aspect for the design and production of such electronic devices. Low cost, energy efficient, mercury-free, long lifetimes, and compactness are the main advantages of LEDs [1]. There are two approaches to white light generation with LEDs: 1) phosphor based white LEDs, and 2) multi-coloured LED solutions – including RGB-LEDs. Presently, commercial white LEDs available in the market use a coating of Ce^{3+} activated yttrium aluminium garnet ($Ce^{3+}:Y_3Al_5O_{12}$, Ce:YAG) phosphor on a blue LED chip of GaN or InGaN. The white light is generated by a combination of the non-absorbed blue emission from the blue LED and the broad yellow emission from Ce:YAG phosphor [2]. However, it inherently suffers from a low colour-rendering index due to the red spectral deficiency [3–5]. Many researchers are studying how to modify Ce:YAG, i. e. co-doping the garnet phase to obtain a phosphor with ideal optical properties that has a broad emission band covering the green and red regions in the blue-light excitation [6–8]. As an alternative, Ce:YAG ceramics and polymeric composites were also investigated. Recently, some of us demonstrated that polymeric composites of polymetylmethacrylate (PMMA) containing Ce:YAG is an ideal yellow light emitter complementary to a blue light to the realization of a white LED on a large scale [9–11].

In this paper, we investigated the effect of the amount of Ce:YAG on the optical properties of a Ce:YAG-PMMA composite. The composites were also combined with a blue LED to investigate the effect of the amount of Ce:YAG on the colour of the emitted light. Ce:YAG-PMMA composites were prepared by using melt compounding at different compositions (0–5 wt. % of Ce:YAG). The optical properties were measured by using photoluminescence spectroscopy. X-ray diffraction (XRD), transmission electron microscopy (TEM) and ^{13}C cross-polarization magic-angle spinning NMR ($^{13}C\{^1H\}$ CP-MAS NMR) were used to investigate the structure, morphology and interaction between the two components.

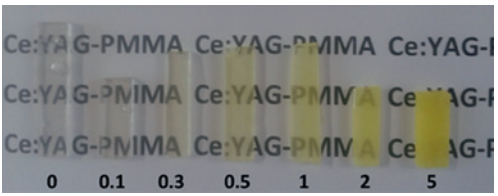

Figure 1: Photo of the obtained composites at different Ce:YAG amount (0–5 wt. %).

2 Materials and methods

2.1 Materials

Ce:YAG powder, with a density of 4.8 g cm^{-3}, was supplied by Dogtai Tianyuan Fluorescent Materials, China. Commercial grade PMMA (Altuglas (â) V920T), in pellet form, having a melt flow rate of 1 g/10 min at 230 °C/3.8 kg, M_w = 110 000 g mol^{-1}, produced by Altuglas International (France).

2.2 Preparation of the Ce:YAG-PMMA composites

PMMA pellets and Ce:YAG powder were dried in an oven at 80 °C for 12 h before use. All composites were prepared by mixing the polymer and filler in a Brabender Plastograph 50 mL internal mixer at 200 °C and 50 rpm for 10 min. For the preparation of the composites, PMMA was first melted for 2 min at 200 °C, and different amount (0.1, 0.3, 0.5, 1, 2 and 5 wt. %) of the Ce:YAG were added into the molten polymer and mixed for a further 8 min. The samples were then melt pressed into 3 mm thick sheets at 200 °C for 5 min at 50 bar. Pure PMMA, as a control sample, was prepared following the same procedure. Yellow solid products, composed of the PMMA polymeric matrix containing Ce:YAG particles, were obtained (Figure 1). The composites remained transparent up to 2 wt. % of Ce:YAG.

2.3 Characterization techniques

The emission (PL) and excitation spectra were measured using a Fluoromax 4 HORIBA Jobin Yvon spectrofluometer. Samples, placed at 45°, were excited by an Xe source operating at 150 W. The Ce:YAG-PMMA composites were excited with a wavelength of 450 nm for emission measurement and 550 nm for excitation measurements.

The emission spectra of the Ce:YAG-PMMA composites combined with a blue LED (InGaN, Quantum Light technology, Voltage 3.2 V, Current 350 mA) were

measured using an Ocean Optics USB2000+XR1 spectrometer operating in the wavelength range 200–1100 nm. The chromaticity coordinates were calculated from the emission spectra following the standard CIE 15:2004.

The X-ray diffraction (XRD) patterns were recorded with a Philips diffractometer in the Bragg–Brentano geometry using a Ni filtered Cu K_α radiation (λ = 1.54056 Å) and a graphite monochromator in the diffracted beam. The X-ray generator worked at 40 kV and 30 mA; the instrument resolution (divergent and antiscatter slits of 0.5°) was determined using standards free from the effect of reduced crystallite size and lattice defects.

The transmission electron microscopy (TEM) micrographs were acquired using a JEM-2100 (JEOL, Japan) electron microscope operating at 200 kV accelerating voltage. For the observation of the composites, 100 nm thick slices were prepared by using a Leica EM UC6 ultra-microtome, and were put onto a 3 mm Cu grid 'lacey carbon' for analysis.

The $^{13}C\{^1H\}$ CP-MAS NMR spectra were obtained at room temperature using a Bruker Avance II 400 MHz (9.4T) spectrometer operating at 100.63 MHz for the ^{13}C nucleus with a MAS rate of 10 kHz, 400 scans, a contact time of 1.5 μs, and a repetition delay of 2 s. The optimization of the Hartmann-Hahn condition was obtained using an adamantane sample. Each sample was placed in a 4 mm zirconia rotor with KEL-F caps using silica as filler to avoid inhomogeneities inside the rotor. The proton spin–lattice relaxation time in the rotating frame $T_{1\rho}(H)$ was indirectly determined, with the variable spin lock (VSL) pulse sequence, by the carbon nucleus observation using a 90°-τ-spin-lock pulse sequence prior to cross polarization with a delay time τ ranging from 0.01 to 3 s. The ^{13}C spin–lattice relaxation time in the rotating frame $T_{1\rho}(C)$ was determined, with the variable spin lock (VSL) pulse sequence, applying the spin-lock pulse after the cross-polarization on the carbon channel. The data acquisition was performed by ^1H decoupling with a spin lock pulse length, τ, ranging from 0.4 to 30 ms and a contact time of 1.5 ms.

3 Results and discussion

The excitation and emission spectra of Ce:YAG powder, of PMMA and of Ce:YAG-PMMA composites, measured at room temperature, are reported in Figure 2.

The excitation spectrum of the Ce:YAG powder show a large band centered at 460 nm and assigned to the $2F_{5/2} \rightarrow 5d_2$ absorption transition, as expected. No band is observed in the pure PMMA. The excitation spectra of the Ce:YAG-PMMA composites show the same large band which intensity increase with an increase in the amount of Ce:YAG.

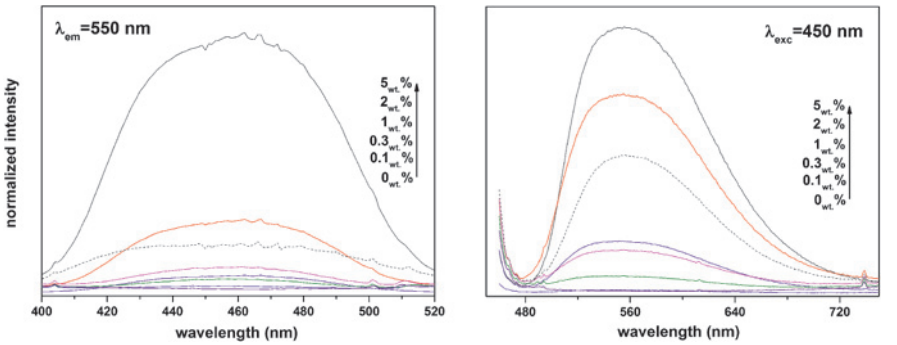

Figure 2: Excitation (left) and emission (right) spectra of Ce:YAG powder (dash), PMMA and Ce:YAG-PMMA composites (lines).

The emission spectra of the powder and of the composites were recorded using λ_{exc} = 450 nm as excitation wavelength which well matches the lowest energy $5d_1$ band of Ce^{3+}. In all case, the asymmetric spectra consist of a very broad band located around 550 nm associated with the 5d(2A1g) → 4f ($2F_{5/2}$ and $2F_{7/2}$) transitions of Ce^{3+}. No band is observed in the pure PMMA. In the composites, the band intensity increases with the amount of Ce:YAG. Since it is well known that the luminescent intensity is related to the average distance between luminescent centres [11], this could be due to the concentration of Ce:YAG in the polymer. The Ce:YAG-PMMA composites loaded with 0.5 and 5 wt. % Ce:YAG were, thus, analyzed with TEM to investigate the distribution of the particles in the polymer. Some of the TEM micrographs, taken at different magnifications, of the Ce:YAG-PMMA composites loaded with 0.5 and 5 wt. % Ce:YAG are shown in Figure 3.

The Ce:YAG particles maintained the same mean size (~ 0.5 μm) in all the analysed samples. Being the filler commercially available, and knowing that the particles size of the filler is of few μm (polydispersion in the range 0.1–2 μm), it is possible to assert that the size of the filler is not influenced by the preparation method we used.

The particles formed clusters uniformly dispersed in the composite, but their distribution was significantly different. For the 0.5 wt. % composite, isolated clusters were present, while for the 5 wt. % composite a more homogeneous dispersion of clusters was observed.

However, the maximum emission wavelength (λ_{max}) significantly changed and a shift of 15 nm was observed increasing the Ce:YAG amount, as reported in Figure 4. The value of λ_{max} of the Ce:YAG-PMMA loaded at 2 and 5 wt. % is equal to the ones of the Ce:YAG powder.

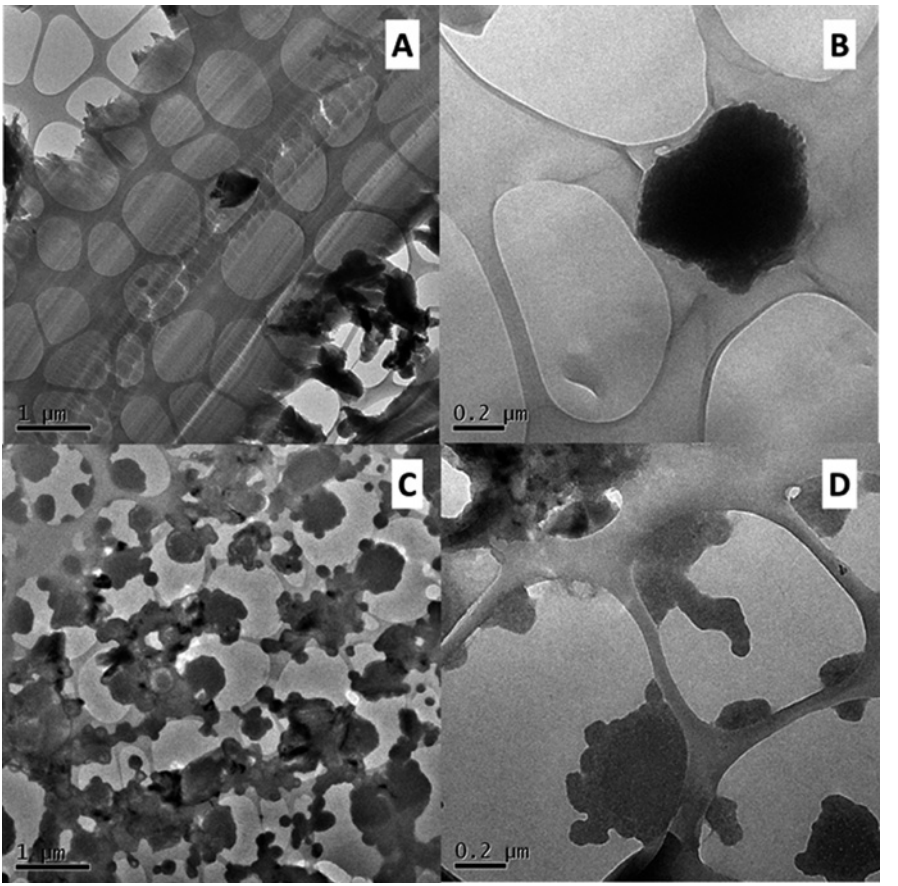

Figure 3: TEM micrographs of Ce:YAG-PMMA composites (A–B) 0.5 wt. % (C–D) 5 wt. % at two magnifications.

This finding cannot to be ascribed to any significant shifts of the excitation bands, indicating that the shift of the emission band does not come from any significant variations in the energy position of the 5d electronic states of the Ce^{3+} ions, both in terms of their population and type. Since the shift could be ascribed to changes in the cell parameters of the garnet phase and in the crystal field around the Ce^{3+} ions, XRD patterns of the Ce:YAG, PMMA and the Ce:YAG-PMMA composites were obtained and reported in Figure 5.

The diffraction pattern of the Ce:YAG powder is typical for the garnet phase. The diffraction pattern of PMMA shows a broad diffraction peak band centred around 14°, typical of an amorphous material, together with two bands of lower intensities centred at 29.7° and 41.7°, in line with previously reported results [12–

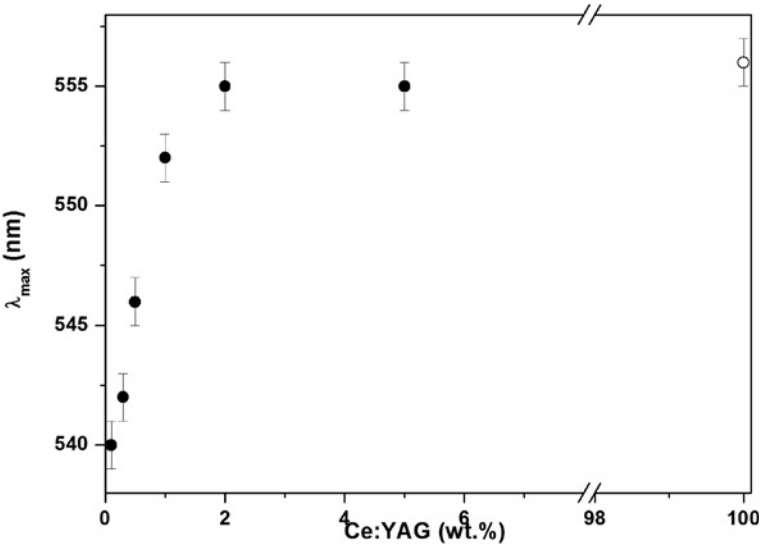

Figure 4: Position of the maximum of the emission band of the Ce:YAG powder (○) and of Ce:YAG-PMMA composites (●) as function of Ce:YAG amount.

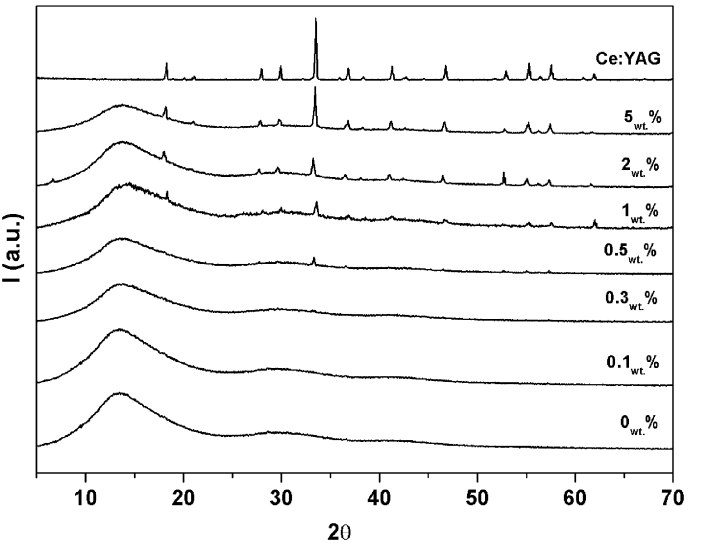

Figure 5: XRD patterns of Ce:YAG, PMMA and Ce:YAG-PMMA composites.

15]. The first band reflects the ordered packing of polymer chains while the second and third one denote the ordering inside the main chains with their intensity systematically decreasing [16]. The diffraction pattern of the composites loaded with 0.1 and 0.3 wt. % are similar to that of the pure PMMA. A low intensity diffraction peak appears at 33° in the pattern of the composite loaded with 0.5 wt. % Ce:YAG. All the peaks of the garnet phase, with intensities increasing with increasing amount of Ce:YAG, are present in the XRD patterns of the composites loaded with 1, 2 and 5 wt. % Ce:YAG. No shift in the position of the garnet phase peaks with respect to the powder was observed, thus confirming that no structural modification occurred in the filler when it was embedded in the polymer. No change in the cell parameter of the garnet phase was observed, indicating that the observed shift in the emission band is attributable to the different environment around the Ce:YAG particles. Bhat et al. [17] demonstrated that the emission bands of phosphors can be tuned by varying the optical properties of the matrix. In our opinion, on the basis of these speculations, the observed shift was probably the result of specific interactions between the polymer chains and the Ce:YAG filler particles.

$^{13}C\{^{1}H\}$ CP-MAS NMR measurements were performed to understand the possible changes of the polymeric chains caused by the presence of Ce:YAG in the polymer and to investigate the interactions between the two components. The $^{13}C\{^{1}H\}$ CP-MAS NMR spectra of PMMA and the Ce:YAG-PMMA composites, and the assignment of the ^{13}C chemical shifts of the polymer are reported in Figure 6.

All the spectra show five resonance peaks at 177.9, 55.4, 52.3, 45.2 and 16.6 ppm due to respectively the carbonyl carbon, methoxyl group, the quaternary carbon of the polymer chain, and the methylene and methyl groups. No modification in the chemical shift and in the signal shape was observed in the presence of Ce:YAG. This confirmed that there were no chemical interactions and that only physical interactions occurred between the polymer and the Ce:YAG particles.

In order to investigate possible molecular interactions between the components, and to detect dynamic changes in the polymer induced by the presence of Ce:YAG, the proton and carbon spin lattice relaxation times in the rotating frame, $T_{1\rho}(H)$ and $T_{1\rho}(C)$, were determined through solid-state NMR measurements. Both the $T_{1\rho}(H)$ and $T_{1\rho}(C)$ values give information about molecular motions in the kHz range [18–20]. These motions reflect the dynamic behaviour of a polymeric chain in a range of a few nanometers. However, for natural-abundance experiments the spin diffusion is less effective in the $T_{1\rho}(C)$ averaging, and this parameter is therefore a good probe for local mobility. The $T_{1\rho}(H)$ and $T_{1\rho}(C)$ values obtained from each peak in the ^{13}C spectra of all the samples are reported in Table 1.

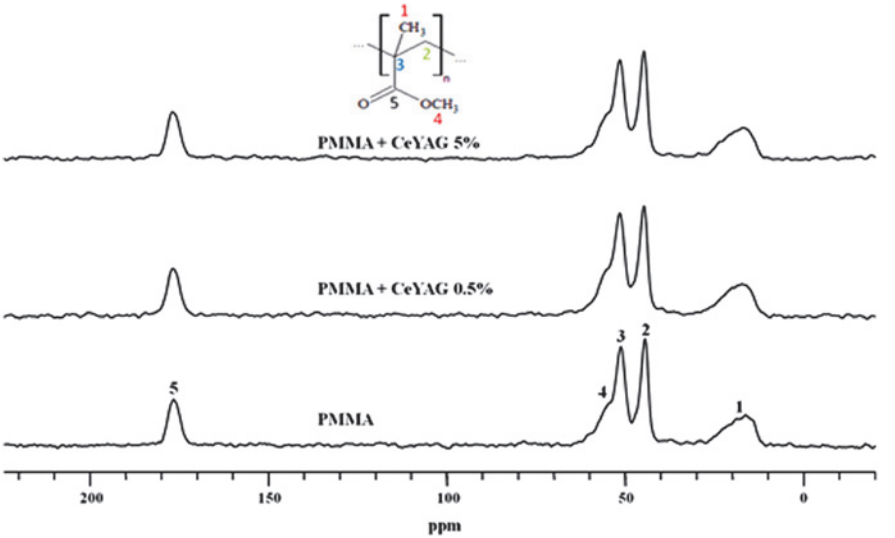

Figure 6: $^{13}C\{^{1}H\}$ CP-MAS NMR spectra of PMMA and of Ce:YAG-PMMA composites.

Table 1: Relaxation time values for all the peaks in the ^{13}C spectra of PMMA and of Ce:YAG-PMMA composites loaded with 0.5 and 5 wt. % Ce:YAG.

Carbon	ppm	$T_{1\rho}H$ (ms)			$T_{1\rho}C$ (ms)		
		PMMA	Ce:YAG-PMMA (0.5 wt. %)	Ce:YAG-PMMA (5 wt. %)	PMMA	Ce:YAG-PMMA (0.5 wt. %)	Ce:YAG-PMMA (5 wt. %)
1	177.9	14.3 ± 0.2	16.1 ± 0.2	33.5 ± 0.2	30.1 ± 0.3	24.8 ± 0.2	16.4 ± 0.3
2	55.4	–	21.5 ± 0.2	–	41.0 ± 0.2	4.6 ± 0.4	6.4 ± 0.3
3	52.3	20.5 ± 0.1	11.8 ± 0.1	54.4 ± 0.3	62.6 ± 0.4	10.7 ± 0.2	10.6 ± 0.2
4	45.2	13.4 ± 0.1	9.5 ± 0.3	15.8 ± 0.2	65.3 ± 0.2	14.9 ± 0.2	16.2 ± 0.1
5	16.6	15.2 ± 0.2	15.7 ± 0.4	10.6 ± 0.3	17.0 ± 0.1	19.6 ± 0.2	24.4 ± 0.2

The calculated $T_{1\rho}(H)$ values for all the peaks in PMMA are of the same order of magnitude. The similar relaxation times for the proton bound to the corresponding carbon atoms indicate that no specific interactions occurred. As a consequence, the material can be considered homogeneous to the length scale of a few nanometers. The loading of 0.5 wt. % Ce:YAG in PMMA does not cause any appreciable change to the above parameter, thus indicating that this concentration is unable to modify the dynamic behaviour of the polymer. Different behaviour was observed for the composite loaded with 5 wt. % Ce:YAG, where the $T_{1\rho}(H)$ values were strongly affected by the presence of the filler. There was an obvious

increase in the $T_{1\rho}$(H) values for signals 1 and 3, compared to the ones of the pure PMMA. These longer relaxation times can be ascribed to a local stiffness (within a few nanometer length) as a result of the presence of the filler.

The calculated $T_{1\rho}$(C) values vary a lot between the different samples and relaxation peaks, and there is no trend. However, for both composites these values were strongly affected by the presence of the Ce:YAG particles. This indicates that a minor contribution to the $T_{1\rho}$ relaxation arises from each molecular group that modulates the $^{1}H-^{13}C$ dipolar coupling. A bigger decrease was observed for the 2, 3 and 4 carbons. These variations can account for specific interactions between the polymer and the surfaces of the Ce:YAG particles. In fact, in agreement with a previous finding [9, 10], an electron donor-acceptor interaction between the carboxyl oxygen lone pair and the surface yttrium or cerium ions could take place. This specific interaction can account for the observed variations in the relaxation time due to the retrieval of electrons along the polymer chain. This finding could also account for the more homogenous composite, as demonstrated by TEM, and for the shift observed in the emission spectra, and these interactions can modify the probability of an electron transition between the electronic states.

The Ce:YAG-PMMA composites were combined with a blue LED in order to test the composite efficiency and to verify its potential use as a white light source. The emission spectra and the relative CIE 1931 colour space of the resulting lights are reported in Figures 7A and 7B, respectively.

The emission spectrum of the resulting light constitutes of two bands. The first, centred at 450 nm, is due to the blue LED, and the second one, centred at 550 nm, is due to the emission of the composite. The results show that by increasing the amount of Ce:YAG in the composite, the emission intensity at 450 nm decreased, while that at 550 nm increased.

The chromaticity coordinates, calculated from the emission spectra of the resulting lights, are reported in the Commission Internationale de l'Eclairage (CIE) chromaticity diagram (Figure 7B). The CIE (x, y) coordinates of the lights obtained combining the blue LED with the composites loaded with up to 2 wt. % Ce:YAG are located in the blue region. Those of the lights obtained combining the blue LED with the composites loaded with 5 wt. % Ce:YAG are located in the white region. This composite is therefore more suitable for a white LED device. The reason of the observed behaviour could be ascribed to better balance of light between the emission from blue LEDs and the emissions from phosphor necessary to obtain white light with proper colour rendering index and colour temperature [21]. The higher intensity of the emission of the Ce:YAG-PMMA loaded with 5 wt. % and the observed shift in the maximum of the band are the responsible of the better matching with the blue light of LED. This means that the good dispersion observed

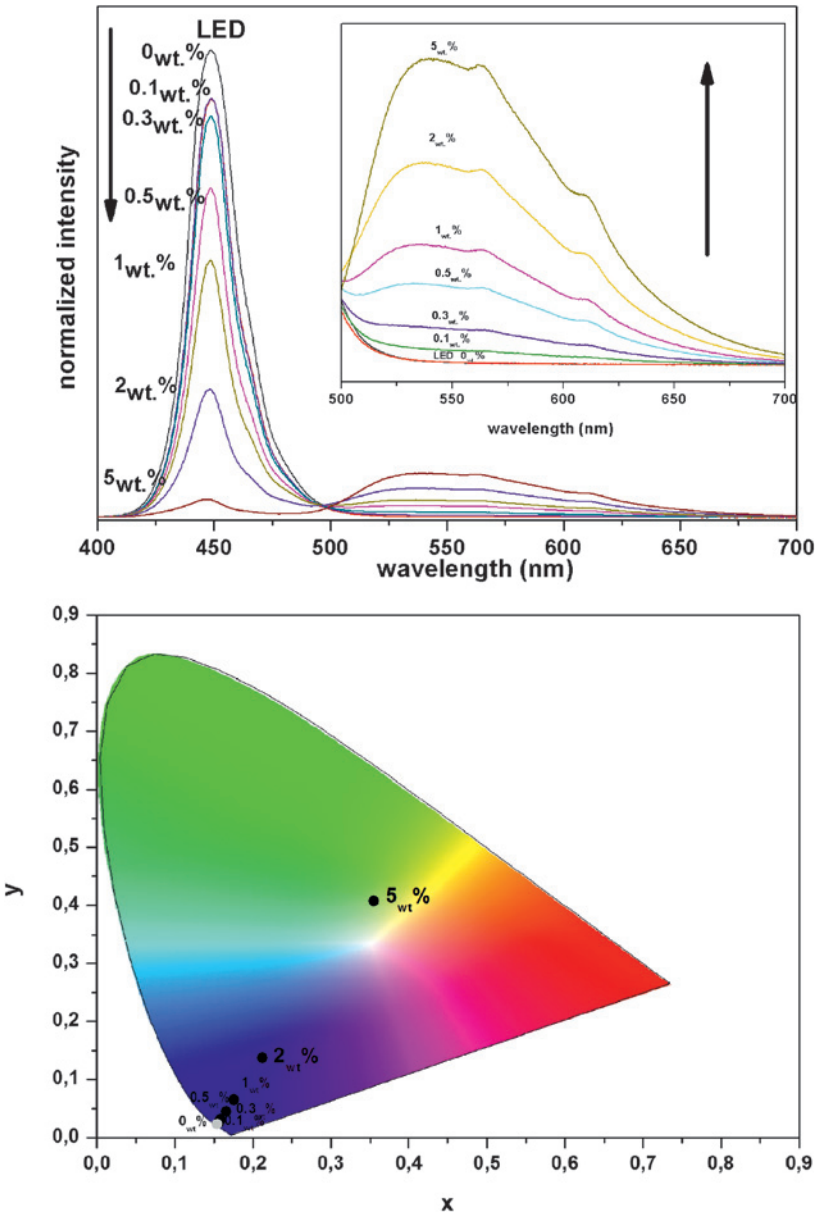

Figure 7: (A) Emission spectra and (B) and the relative CIE 1931 colour space of the resulting light.

by TEM and the specific interactions investigated with NMR influenced the resulting light.

4 Conclusions

A series of Ce:YAG-PMMA composites were prepared by melt compounding. The effect of the amount of Ce:YAG on the structure, morphology and optical properties of the composites was investigated. The results show that the particles are well dispersed in the polymer. The polymer is amorphous and the crystalline phase of Ce:YAG does not change in the composite. When increasing the amount of Ce:YAG, a shift in the emission spectrum occurred. This behaviour was ascribed to electron donor-acceptor interactions between the carboxyl oxygen lone pair and the particle surface, as indicated by the changes in the relaxation times obtained by NMR.

The combination of the composites with blue LED gives the best white light for the Ce:YAG-PMMA composite loaded with 5 wt. % Ce:YAG. In this case, the obtained light better balances the light between the emission from blue LEDs and the emissions from Ce:YAG. The result clearly shows that the colour properties of light from white LEDs can be controlled by an appropriate selection of the phosphor in a composite.

Acknowledgement: The authors acknowledge the University of Palermo, FFR 2012–2013 –ATE 0594 "Development of new methodologies for the synthesis and functionalization of nanoparticles with luminescence properties for advanced applications" and CORI2013 (Bando per la concessione di contributi per l'avvio e lo sviluppo di collaborazioni dell'Ateneo 2013 – Azione D – prot. 32827 del 2/5/2013). NMR and TEM experimental data were provided by Centro Grandi Apparecchiature – UniNetLab – Università di Palermo funded by P.O.R. Sicilia 2000–2006, Misura 3.15 Azione C Quota Regionale. Student support was provided by the National Research Foundation in South Africa. Thanks to Dr. Camillo Sartorio for the registration of the excitation and of the emission spectra.

References

1. R. Zhang, H. Lin, Y. Yu, D. Chen, J. Xu, and Y. Wang, Laser Photonics Rev. **8** (2014) 158 and reference therein.
2. G. Blasse and A. Bril, J. Chem. Phys., **47** (1967) 5139.

3. J. K. Kim, H. Luo, E. F. Schubert, J. Cho, C. Sone, and Y. Park, Jpn. J. Appl. Phys. **44** (2005) L649.
4. V. Tucureanu, A. Matei, I. Mihalache Mihai Danila, M. Popescu, and B. Bita, J. Mater. Sci. **50** (2015) 1883.
5. M. Kottaisamy, P. Thiyagarajan, J. Mishra, and M. S. Ramachandra Rao, Mater. Res. Bull. **43** (2008) 1657.
6. A. B. Muñoz-García, J. L. Pascual, Z. Barandiarán, and L. Seijo, Phys. Rev. B **82** (2010) 064114.
7. M. Upasani, B. Butey, and S. V. Moharil, J. Appl. Phys. **6** (2014) 28.
8. J. Chen, Z. Deng, Z. Liu, Y. Lin, H. Lan, D. Chen, and Y. Cao, Opt. Express **23** (2015) A292.
9. M. L. Saladino, A. Zanotto, D. F. Chillura Martino, A. Spinella, G. Nasillo, and E. Caponetti, Langmuir **26** (2010) 13442.
10. M. L. Saladino, D. F. Chillura Martino, M. A. Floriano, D. Hreniak, L. Marciniak, W. Stręk, and E. Caponetti, J Phys. Chem C **118** (2014) 9107.
11. M. L. Saladino, F. Armetta, M. Sibeko, A. S. Luyt, D. F. Chillura Martino, and E. Caponetti, J. Alloy. Compd. **664** (2016) 726.
12. M. L. Saladino, T. E. Motaung, A. S. Luyt, A. Spinella, G. Nasillo, and E. Caponetti, Polym. Degrad. Stabil. **97** (2012) 452.
13. T. E. Motaung, A. S. Luyt, F. Bondioli, M. Messori, M. L. Saladino, A. Spinella, and E. Caponetti, Polym. Degrad. Stabil. **97** (2012) 1325.
14. T. E. Motaung, A. S. Luyt, M. L. Saladino, D. F. Chillura Martino, and E. Caponetti, Express Polym. Lett. **6** (2012) 871.
15. V. K. Thakur, D. Vennerberg, S. A. Madboulyb, and M. R. Kessler, RSC Adv. **4** (2014) 6677.
16. E. Shobhana, Int. J. Mod. Eng. Res. **2** (2012) 1092.
17. S. V. Bhat, A. Govindaraj, A., and C. N. R. Rao, Chem. Phys. Lett. **422** (2006), 323.
18. T. E. Motaung, M. L. Saladino, A. S. Luyt, and D. F. Chillura Martino, Compos. Sci. Technol. **73** (2012) 34.
19. T. E. Motaung, A. S. Luyt, M. L. Saladino, and E. Caponetti, Polym. Composite. **34** (2013) 164.
20. T. E. Motaung, M. L. Saladino, A. S. Luyt, A. S., and D. F. Chillura Martino, Eur. Polym. J. **49** (2013) 2022.
21. L. Lei Chen, C.-C. Lin, C.-W., Yeh, and R.-S. Liu, Materials **3** (2010) 2172.